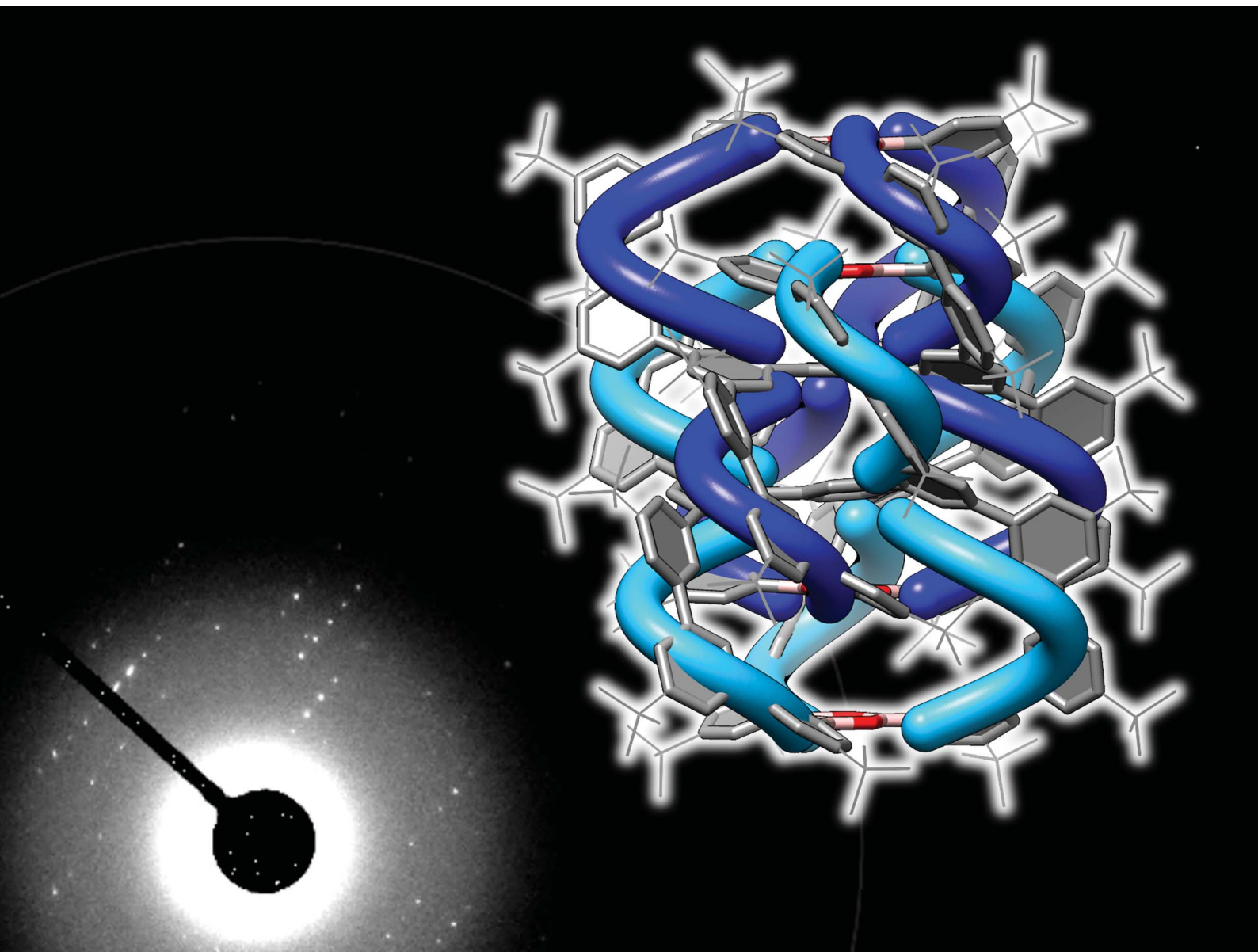


Chemical Science

rsc.li/chemical-science



ISSN 2041-6539

Cite this: *Chem. Sci.*, 2025, **16**, 19594

All publication charges for this article have been paid for by the Royal Society of Chemistry

Received 11th September 2025
Accepted 7th October 2025DOI: 10.1039/d5sc06999h
rsc.li/chemical-science

Introduction

The geometry of three-dimensional nets is crucial in understanding space-filling structures in nature and intersects with various disciplines such as chemistry, crystallography, materials science and mathematics.^{1,2} Carbonaceous nets of sp^3 -hybridized carbon atoms, for instance, reveal the geometrical features that support the hardness of diamond³ and unravel the conundrum of cyclohexane structures (Fig. 1).⁴ Studies of diamond segments, polymantanes, further led to advancements in the fundamental and synthetic chemistry of diamondoids.^{5–7} The structure of diamond with a 6^6 -(a) net was found to be strongly isotropic by Sunada, which led him to rediscover the (10,3)-a net as a diamond twin that commonly possesses a strongly isotropic character. The (10,3)-a net was originally discovered by Laves in 1932,^{8,9} and it attracted the interest of researchers from various fields, resulting in various different names such as srs, gyroid and K_4 lattice being given to this unique net.^{1,10} Interestingly, the geometry of the (10,3)-a net is chiral, which also gives rise to unique physical properties of interest.¹¹ Although the chiral (10,3)-a net of sp^2 -hybridized carbon atoms (pollux) has also attracted theoretical interest,^{10,12,13} its presence has been

questioned because of the severe lack of stability.¹⁴ By replacing the sp^2 -hybridized carbon atoms of pollux with phenine (1,3,5-trisubstituted benzene),^{15,16} we recently introduced the first primal cage unit of pollux and named it phenine polluxene (Fig. 1).¹³ As was the case with polymantane,¹⁷ however, expansion of the (10,3)-a net of monopolluxene was challenging, which urged us to develop further synthetic strategies for expanded cages with unique symmetry. In this study, the next homologue of polluxene, *i.e.*, phenine dipolluxene, was synthesized by

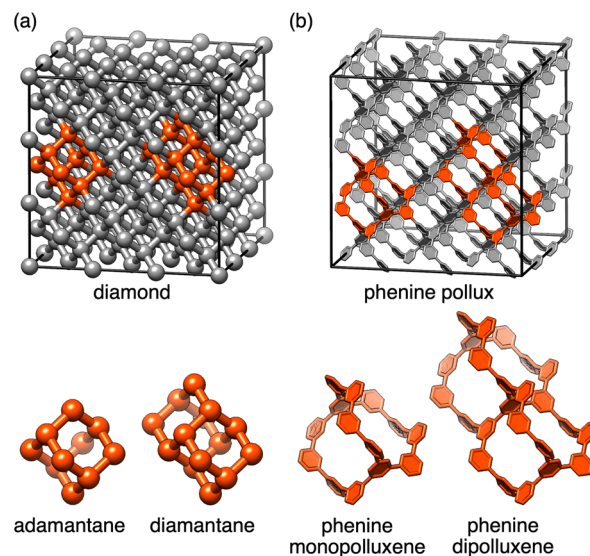


Fig. 1 Strongly isotropic nets of carbon atoms. (a) Diamond and its molecular segments (adamantane and diamantane). (b) Phenine pollux and its molecular segments (monopolluxene and dipolluxene).

^aDepartment of Chemistry, The University of Tokyo, Hongo 7-3-1, Bunkyo-ku, Tokyo 113-0033, Japan. E-mail: isobe@chem.s.u-tokyo.ac.jp

^bRIKEN SPring-8 Center, Kouto 1-1-1, Sayo-cho, Sayo-gun, Hyogo 679-5148, Japan

^cDepartment of Applied Chemistry, The University of Tokyo, Kashiwanoha 6-6-2, Kashiwa, Chiba 277-0882, Japan

^dInstitute of Multidisciplinary Research for Advanced Materials, Tohoku University, Aoba-ku, Sendai, Japan

† Dedicated to Professor Koichi Narasaki on the occasion of his 80th birthday.

‡ Present address: Department of Inorganic Chemistry, University of Vienna, Vienna, Austria.



developing a three-component cross-coupling route for the cage-forming reaction. The chiral cage structure with sextuple helix was unequivocally revealed by crystallography. Unexpectedly, when we analyzed a synthetic precursor of dipolluxene, an interpenetrated dipolluxene dimer was found. Electron crystallographic analyses of the dimer revealed a unique interpenetrated structure with an entangled duodecuple helix with homohelicity.

Results and discussion

Molecular structures and design

Structures and synthetic routes are first described. As shown in Fig. 2, the cage structure of phenine monopolluxene is expanded along the C_3 axis to establish the two-story structure of phenine dipolluxene (**1**) as the next target in the present study. Although these two congeners share a common point symmetry of D_3 with the C_3 and C_2 axes penetrating the cage structures, the difference in the location of the symmetry axes in the cages forced us to revise the synthetic route for the expanded congener. For the previous synthesis of phenine

monopolluxene, one of the C_2 axes was first generated by constructing a 10-membered ring of phenine units, and the other symmetry axes were generated at the final step. The final step for the cage-forming reaction adopted the Ni-mediated Yamamoto coupling to close a transannular bridge *via* an intramolecular cyclization (Fig. 2a). When applied to the two-story congener in this study, this transannular strategy required a precursor with fused 10-membered rings, and this precursor was synthetically demanding. We then noted that a triaryl benzene unit with a preformed C_3 axis at the center was synthetically accessible and could serve as a synthetic precursor (see also **2** in Fig. 3). Although this revised route was also challenging, with six-fold Suzuki-Miyaura coupling of three components at the final step, we decided to adopt this route for the synthesis of phenine dipolluxene. For further details of the retrosynthetic analyses, see the SI (Fig. S1).

Synthesis

The synthesis of phenine dipolluxene **1** is next described (Fig. 3). The triaryl benzene precursor (**2**) was prepared by

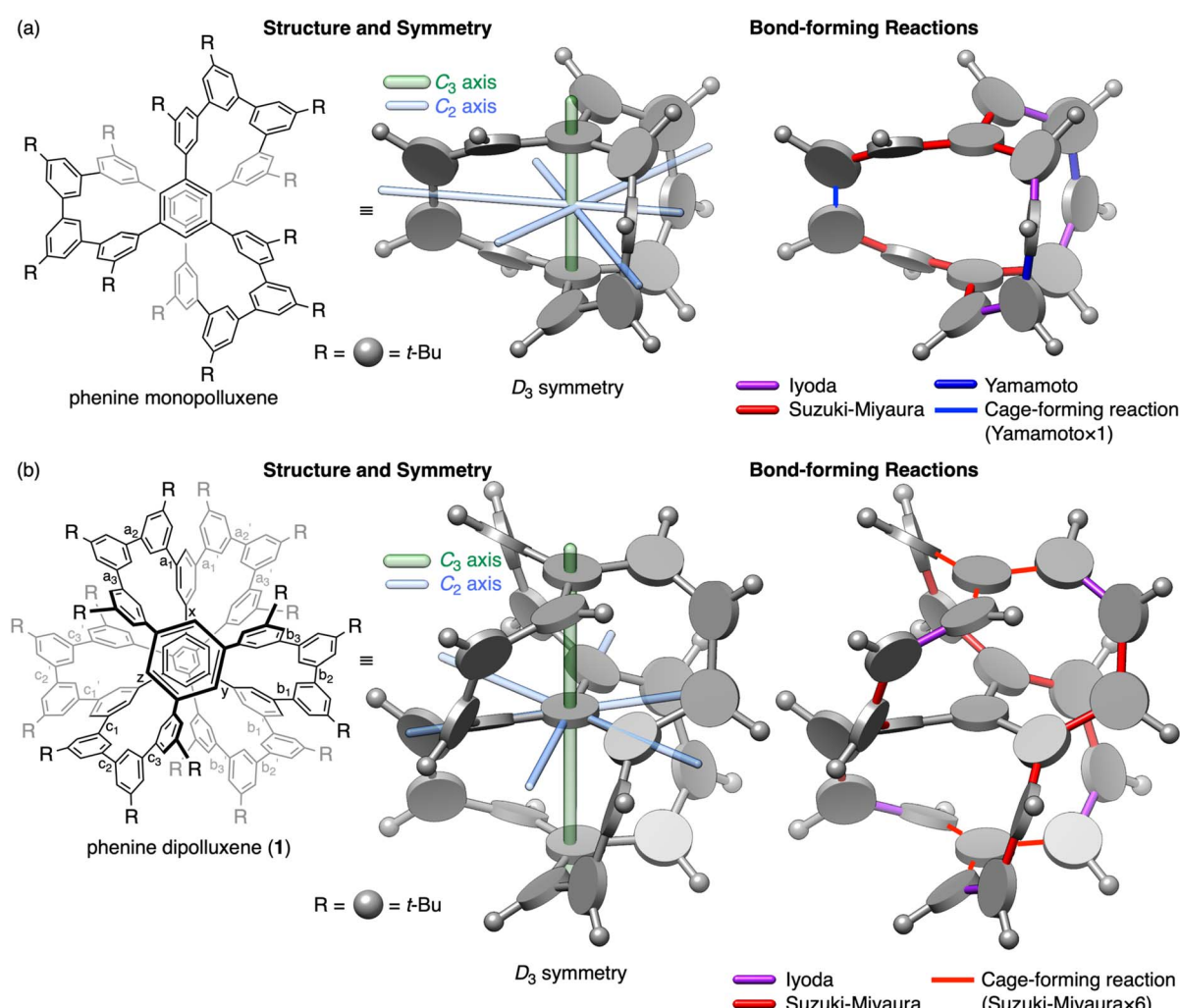


Fig. 2 Structures, symmetry and bond-forming reactions. (a) Phenine monopolluxene. (b) Phenine dipolluxene.



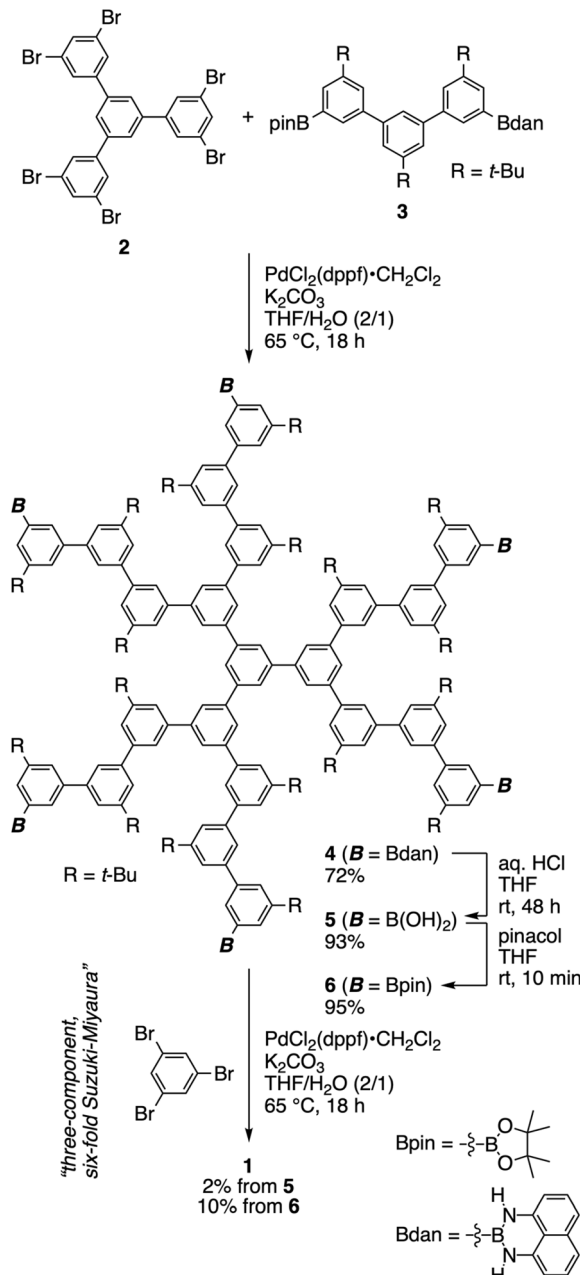


Fig. 3 Synthesis of phenine dipolluxene 1.

methods reported in the literature, and the terphenyl precursor (3) was prepared by a 3-step process consisting of two sets of Suzuki–Miyaura coupling and one set of C–H borylation (see SI for details). The terphenyl precursor (3) was furnished with two different boryl groups (Bpin and Bdan), which allowed us to perform Suzuki–Miyaura coupling on each end of this precursor separately at two different stages. Six-fold Suzuki–Miyaura coupling of 2 with 3 on the Bpin-terminus was thus performed to obtain 4 with six Bdan-termini. After the hydrolysis of Bdan moieties, arylboronic acid 5 was subjected to Suzuki–Miyaura coupling with 1,3,5-tribromobenzene. Although the three-component coupling process involved complicated regioselectivity (Fig. S1), we were pleased to obtain phenine

dipolluxene (1) *via* six-fold Suzuki–Miyaura coupling of 5 with tribromobenzene. However, the yield was not sufficiently high to isolate and identify the compound in full. We then installed pinacol moieties on the boryl groups and performed three-component six-fold Suzuki–Miyaura coupling between 6 and tribromobenzene. The yield improved, and the target, phenine dipolluxene (1), was obtained in 10% yield. As six biaryl linkages were formed during this cage-forming step, the average efficiency of bond formation was ~70% per linkage. We believe that the sterically congested cores, such as those of 5 and 6, possessed a preorganized conformation suitable for three-component covalent assembly (*cf.* Fig. S1). The combination of this three-component coupling strategy with the preceding intramolecular cyclization strategy to form decagonal phenine cycles¹³ should allow for the rational synthesis of expanded cages of polluxenes. As is often the case with phenine nanocarbons, phenine dipolluxene was transparent in the visible-light region (Fig. S3), which could be beneficial for exploration of chiral, electronic materials.¹⁸

Molecular structures

The structure of phenine dipolluxene was unequivocally revealed by X-ray crystallography. As shown in Fig. 4a, the two-story structure of 1 was revealed with six arms forming a homohelical sextuple helix.¹⁹ Adopting systematic names to describe the helicity,^{13,20} one helical arm comprising (S,R,S)-configurations is described as a (*P*)-isomeric structure. The overall sextuple helical structure of 1 can thus be described as (*P,P,P,P,P,P*) to designate the right-handed helicity of the homohelical arms. The crystal of 1 was a racemate, and the enantiomeric pair of (*P,P,P,P,P,P*)- and (*M,M,M,M,M,M*)-isomers was included in the crystal (Fig. S4). Studies on the host-guest chemistry of the multiply arrayed cages should be interesting for explorations of unique properties and functions.^{13,21} As shown in Fig. 4b, an energy barrier of ~11 kcal mol⁻¹ was found for the conformational conversion of the (*P,P,P,P,P,P*)-isomer to the (*M,M,M,M,M,M*)-isomer by rotating the biaryl axes of *x*, *y* and *z* attached to the central phenine unit (see also Fig. S5). Thus, when we rotated the biaryl linkage in a stepwise manner from the relaxed state at (*x*, *y*, *z*) = (33, 33, 33), the energy gradually increased together with the disappearance of the helicity of the rotating arm. When the second arm was rotated from (*x*, *y*, *z*) = (150, 30, 30), the helicity of the three arms disappeared, and the highest energy of +11 kcal mol⁻¹ was recorded. When the third arm was rotated from (*x*, *y*, *z*) = (150, 150, 30), the helicity of the arms gradually emerged to generate the (*M,M,M,M,M,M*)-isomer. The low barrier for this conversion indicated that the enantiomers were rapidly interconverted in solution.

Interpenetrated net

During our investigations to improve the yield of 1, we unexpectedly found that homohelical interpenetrated nets could be realized by adopting phenine design.¹⁵ As noted in the pioneering works of Wells,¹ three-dimensional space can also be filled by interpenetrated nets, which are currently being



 This article is licensed under a Creative Commons Attribution-NonCommercial 3.0 Unported Licence

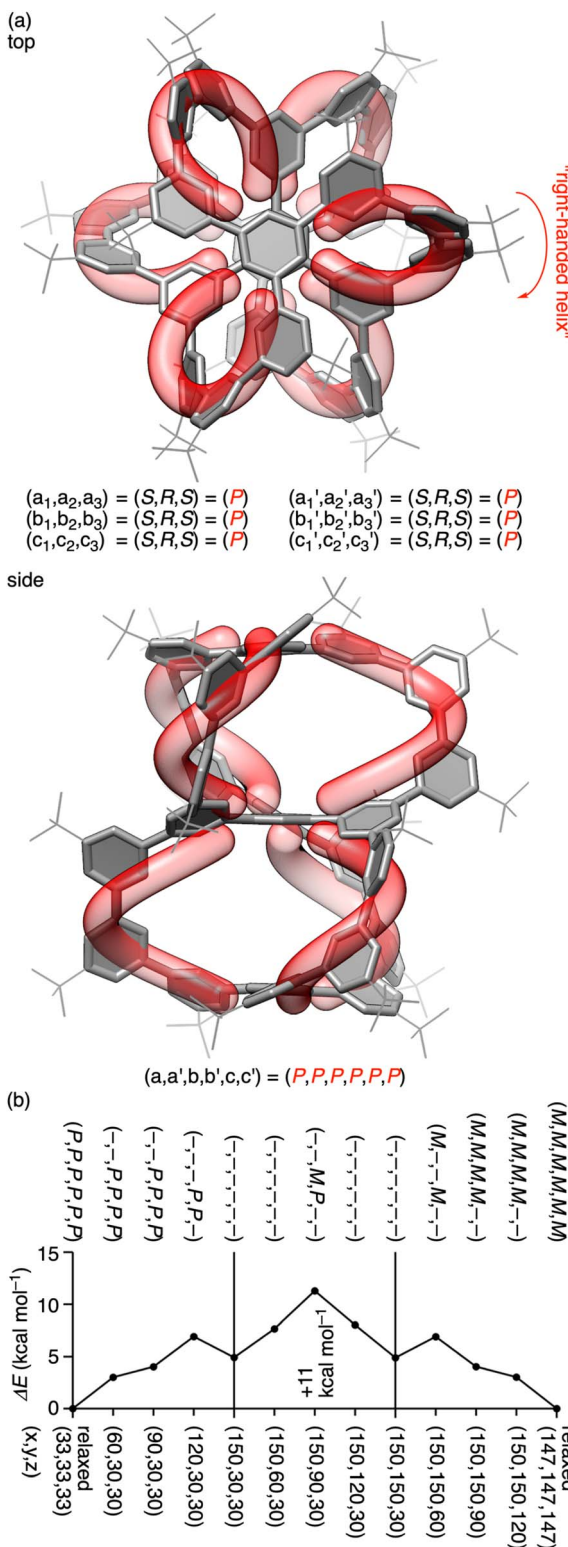


Fig. 4 Structure of phenine dipolluxene (1). (a) Crystal structure. A representative structure of the (*P,P,P,P,P,P*)-isomer is shown. The mirror-image enantiomer, (*M,M,M,M,M,M*), was also found in the crystal of the racemate (Fig. S4). (b) Energetics of the conformers, showing an energy barrier of ~ 11 kcal mol $^{-1}$ between the two enantiomers. Calculations were performed by using a methyl substituted molecule as a model. The helicity of the arms was assigned by adopting a system with (*S,R,S*) = (*P*) and (*R,S,R*) = (*M*), and conformations with other relationships were judged as non-helical and were described as “-”. See also Fig. S5.

exploited by adopting weak bonding such as coordination and/or hydrogen bonds for the assembly.²² Experimentally, the strongly isotropic, chiral net of (10,3)-*a* was first found to form “racemic” interpenetrated nets with heterohelical combinations from coordination polymers and hydrogen bonding networks of lipids.^{23,24} Albeit rare in examples, when the edge unit of coordination polymers was elongated, homohelical combinations of interpenetrated (10,3)-*a* nets was also found from large metal-organic frameworks.²⁵ In this study, we accidentally discovered that the homohelically interpenetrated net of (10,3)-*a* could be formed as a dimeric combination of phenine dipolluxene. While investigating the cage-forming reaction of arylboronic acid 5 in detail, we noted the presence of small crystalline precipitates after the reaction.²⁶ Although we could not obtain a large single crystal suitable for X-ray diffraction experiments, the precipitate was subjected to electron crystallographic analyses with three-dimensional electron diffraction (3D ED) experiments (Fig. S6 and Movie S1).²⁷ For the 3D ED analysis, machine learning-based real-time object locator/evaluator, yoneoLocr, was adopted to locate small crystals and screen their diffractibility for the structural elucidation.²⁸ The crystal structure was unexpectedly complicated and was carefully analyzed. First, the crystal structure from the 3D ED investigation revealed that the dehydration of boronic acid 5 resulted in the formation of BO-hexagonal structures of boroxine (Fig. 5).²⁹ Surprisingly, two dipolluxene molecules were entangled to form an interpenetrated dimer consisting of a homohelical pair such as “(P,P,P,P,P,P) + (P,P,P,P,P,P)” with a duodecuple helix structure (see also Fig. S7). The interpenetrated net resulted from multiple stacks of planar hexagons. At the center, six hexagons consisting of two hydrocarbon units and four BO-doped, boroxine units were stacked in a twisted manner to serve as a stem for twelve helical arms. The twelve helical arms were located in three different locations around the *C*₃ axis, and each location contained stacks of “6 + 4 + 4” hexagons. As a result, the interpenetrated (10,3)-*a* net was formed as an entangled dimer of phenine dipolluxene with the 48 hexagons stacked to form a homohelical assembly of the duodecuple helix. Because the interpenetrated nets were tightly assembled in stacks, the heterohelical racemate would not be readily accessible *via* conformational changes of a single component. We speculate that the stereochemical rigidity may also be acquired in the interpenetrated dimeric entanglement, and properties and functions of chiral phenine nanocarbon should provide interesting subjects to be explored in the future.³⁰ Because of reversible interconversion between boronic acid and boroxine as well as the low solubility of compounds, we could not obtain interpenetrated dipolluxene on a large scale. By designing helical stacks of hexagons, for instance, through donor-acceptor (D-A) pairs, we may design and synthesize chiral interpenetrated polipolluxene in the future. Stacked D-A arrays embedded in a chiral environment of wrapping helical arms would be an interesting structural motif to be exploited in materials science. Additionally, this study demonstrated that the 3D ED analysis with an automated sample screening process could transform synthetic chemistry by enabling the structural elucidation of minor products.²⁸

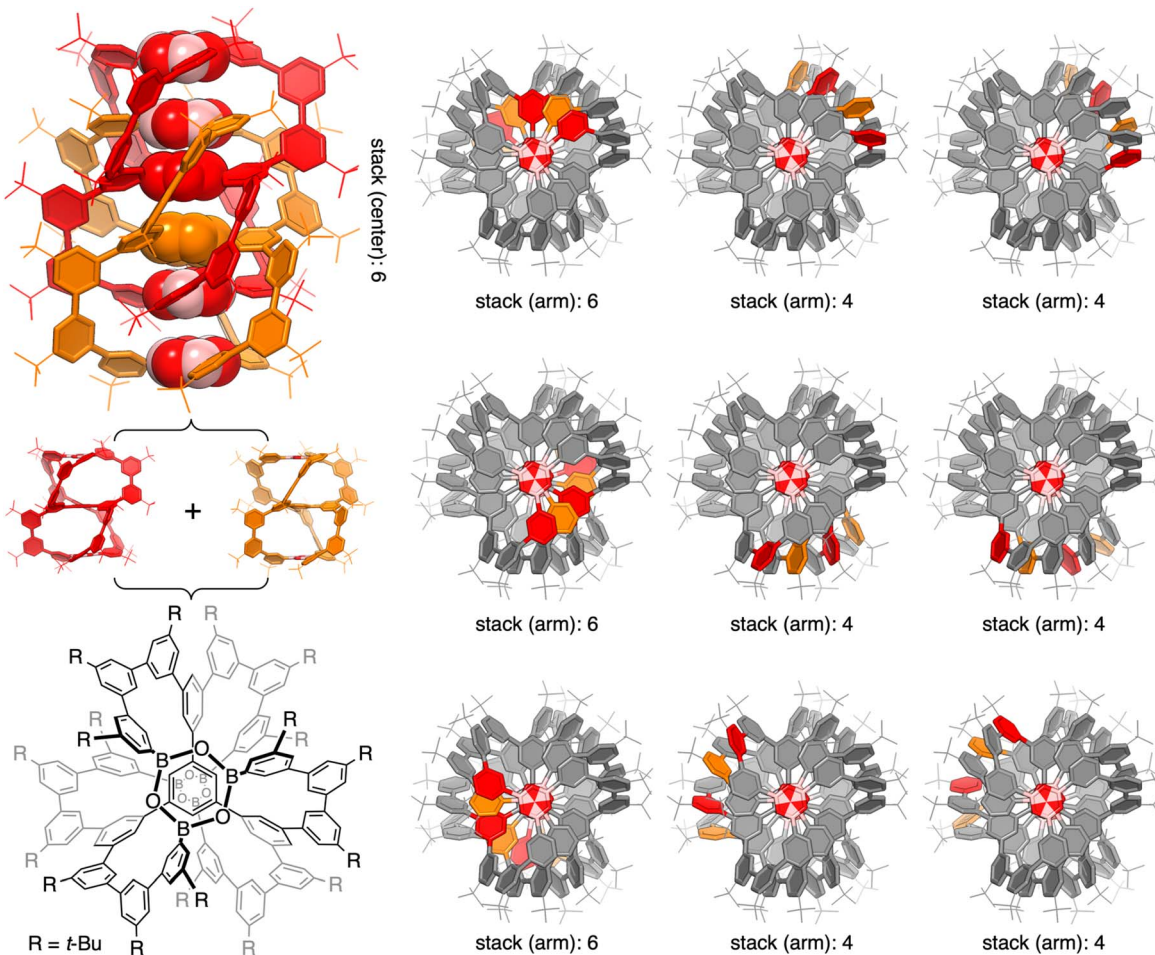


Fig. 5 Interpenetrated BO-doped dipolluxene dimer. Crystal structures were obtained by 3D ED analyses of microcrystalline precipitates obtained from arylboronic acid 5. As a representative structure, an interpenetrated dimeric structure of $(P,P,P,P,P,P) + (P,P,P,P,P,P)$ is shown. See Fig. S7 for further details. In total, 48 stacks of hexagons were found in the structure. Four BO-doped, boroxine hexagons at the center: B = pink, O = red.

Conclusion

In summary, we have expanded the cage structure of polluxene with the $(10,3)\text{-}a$ net by devising a synthetic route exploiting three-component covalent assembly with six-fold Suzuki–Miyaura coupling. The two-story molecular structure was determined by X-ray crystallography to show the presence of a sextuple helix. We found the formation of interpenetrated nets with dipolluxene molecules unexpectedly by examining insoluble precipitates of a synthetic intermediate with the 3D ED analysis. The crystal structure containing BO-doped hexagons was found to possess a homohelical, duodecuple helix, consisting of stacks of 48 hexagons. Although the interpenetrated dimer was accidentally formed, the entangled structure provided an interesting target for the asymmetric synthesis of chiral nanocarbon molecules to be explored in the future. Transformation of phenine stacks, for instance, through high-pressure processes could also be an interesting subject to be investigated.³¹ Notably, a hexagonal structure that is usually conceived as a primal structure of a flatland of graphitic nets

can serve as a primal trigonal planar unit to construct an expanded net of the diamond twin with chirality.^{10,15,16} As suggested by mathematics,¹⁰ chiral, strongly isotropic $(10,3)\text{-}a$ nets can be constructed rationally by trigonal planar structures, with a tolerance of large dihedral angles, even in an expanded and/or entangled manner.

Author contributions

T. M. F.: data curation, formal analysis, funding acquisition, investigation, validation, visualization, writing – original draft, writing – review & editing. K. T.: data curation, investigation, methodology, writing – review & editing. S. Y.: data curation, investigation, methodology, writing – review & editing. S. M.-Y.: data curation, investigation, methodology, writing – review & editing. K. Y.: data curation, investigation, methodology, writing – review & editing. H. I.: conceptualization, formal analysis, funding acquisition, investigation, project administration, validation, visualization, writing – original draft, writing – review & editing.

Conflicts of interest

There are no conflicts to declare.

Data availability

CCDC 2486579 and 2486580 contain the supplementary crystallographic data for this paper.^{32a,b}

The data that support the findings of this study are available in the supplementary information (SI). Supplementary information is available. See DOI: <https://doi.org/10.1039/d5sc06999h>.

Acknowledgements

We wish to thank Professor Roald Hoffmann (Cornell University) for bringing a relevant study to our attention and Dr S. Sato (University of Tokyo) for his help in crystallographic analyses. We were granted access to X-ray diffraction instruments in SPring-8 (BL26B1, no. 2024A1293). This work was partly supported by Sekisui Chemical "Innovation inspired by Nature" Research Support Program, JSPS KAKENHI (25H00003), JST ACT-X (JPMJAX23DI), JST-Mirai (JPMJMI23G2) and AMED Research Support Project for Life Science and Drug Discovery (Basis for Supporting Innovative Drug Discovery and Life Science Research (BINDS); JP23ama121006).

References

- 1 A. F. Wells, *Three-Dimensional Nets and Polyhedra*, Wiley, New York, 1977.
- 2 O. D. Friedrichs, M. O'Keeffe and O. M. Yaghi, Three-Periodic Nets and Tilings: Regular and Quasiregular Nets, *Acta Crystallogr. A*, 2003, **59**, 22–27.
- 3 (a) W. H. Bragg and W. L. Bragg, The Structure of the Diamond, *Nature*, 1913, **91**, 557; (b) W. H. Bragg and W. L. Bragg, The Structure of the Diamond, *Proc. R. Soc. London, Ser. A*, 1913, **89**, 277–291.
- 4 (a) A. Baeyer, Ueber Polyacetylenenverbindungen, *Chem. Ber.*, 1885, **18**, 2269–2281; (b) H. Sachse, Ueber die geometrischen Isomeren der Hexamethylenderivate, *Chem. Ber.*, 1890, **23**, 1363–1370; (c) E. Mohr, Die Baeyersche Spannungstheorie und die Struktur des Diamanten, *J. Prakt. Chem.*, 1918, **98**, 315–353; (d) O. Hassel, Stereochemistry of Cyclohexane, *Q. Rev. Chem. Soc.*, 1953, **7**, 221–230; (e) D. H. R. Barton, The Conformation of the Steroid Nucleus, *Experientia*, 1950, **6**, 316–320.
- 5 (a) S. Landa and V. Macháček, Sur l'Adamantane, Nouvel Hydrocarbure Extrait du Naphte, *Collect. Czech. Chem. Commun.*, 1933, **5**, 1–5; (b) J. E. Dahl, S. G. Liu and R. M. K. Carlson, Isolation and Structure of Higher Diamondoids, Nanometer-Sized Diamond Molecules, *Science*, 2002, **299**, 96–99.
- 6 V. Prelog, Conformation and Reactivity of Medium-Sized Ring Compounds, *Pure Appl. Chem.*, 1963, **6**, 545–560.
- 7 (a) V. Prelog and R. Seiwerth, Über die Synthese des Adamantans, *Chem. Ber.*, 1941, **74**, 1644–1648; (b) P. R. Schleyer, A Simple Preparation of Adamantane, *J. Am. Chem. Soc.*, 1957, **79**, 3292; (c) C. Cupas and P. R. Schleyer, Congressane, *J. Am. Chem. Soc.*, 1965, **87**, 917–918.
- 8 F. Laves, Zur Klassifikation der Silikate. Geometrische Untersuchungen Möglicher Silicium-Sauerstoff-Verbände als Verknüpfungsmöglichkeiten Regulärer Tetraeder, *Z. Krist.*, 1932, **82**, 1–14.
- 9 S. T. Hyde, M. O'Keeffe and D. M. Proserpio, A Short History of an Elusive Yet Ubiquitous Structure in Chemistry, Materials, and Mathematics, *Angew. Chem., Int. Ed.*, 2008, **47**, 7996–8000.
- 10 T. Sunada, Crystals that Nature Might Miss Creating, *Not. Math. Soc.*, 2008, **55**, 206–215.
- 11 (a) J. A. Dolan, B. D. Wilts, S. Vignolini, J. J. Baumberg, U. Steiner and T. D. Wilkinson, Optical Properties of Gyroid Structured Materials: From Photonic Crystals to Metamaterials, *Adv. Opt. Mater.*, 2015, **3**, 12–32; (b) A. Mizuno, Y. Shuku and K. Awaga, Recent Developments in Molecular Spin Gyroid Research, *Bull. Chem. Soc. Jpn.*, 2019, **92**, 1068–1093.
- 12 M. Itoh, M. Kotani, H. Naito, T. Sunada, Y. Kawazoe and T. Adschiri, New Metallic Carbon Crystal, *Phys. Rev. Lett.*, 2009, **102**, 055703.
- 13 (a) T. M. Fukunaga, T. Kato, K. Ikemoto and H. Isobe, A Minimal Cage of A Diamond Twin with Chirality, *Proc. Natl. Acad. Sci. U. S. A.*, 2022, **119**, e2120160119; (b) T. M. Fukunaga, Y. Onaka, T. Kato, K. Ikemoto and H. Isobe, Stoichiometry Validation of Supramolecular Complexes with A Hydrocarbon Cage Host by van 't Hoff Analyses, *Nat. Commun.*, 2023, **14**, 8246.
- 14 Y. Yao, J. S. Tse, J. Sun, D. D. Klug, R. Martoňák and T. Iitaka, Comment on "New Metallic Carbon Crystal", *Phys. Rev. Lett.*, 2009, **102**, 229601.
- 15 (a) M. Faraday, On New Compounds of Carbon and Hydrogen, and on Certain Other Products Obtained during the Decomposition of Oil by Heat, *Phil. Trans.*, 1825, **115**, 440–466; (b) A. Laurent, Sur la Chlorophénise et les Acides Chlorophénisique et Chlorophénésique, *Ann. Chem. Phys.*, 1836, **63**, 27–45; (c) A. Kekulé, Sur la Constitution des Substances Aromatiques, *Bull. Mem. Soc. Chir. Paris*, 1865, **2**, 98–111; (d) A. Kekulé, Ueber einige Condensationsprodukte des Aldehyds, *Ann. Chem. Pharm.*, 1872, **162**, 77–124.
- 16 K. Ikemoto, T. M. Fukunaga and H. Isobe, Phenine Design for Nanocarbon Molecules, *Proc. Jpn. Acad., Ser. B*, 2023, **99**, 335–351.
- 17 R. C. Fort and P. R. Schleyer, Adamantane: Consequences of the Diamondoid Structure, *Chem. Rev.*, 1964, **64**, 277–300.
- 18 (a) J. Y. Xue, T. Izumi, A. Yoshii, K. Ikemoto, T. Koretsune, R. Akashi, R. Arita, H. Taka, H. Kita, S. Sato and H. Isobe, Aromatic Hydrocarbon Macrocycles for Highly Efficient Organic Light-emitting Devices with Single-layer Architectures, *Chem. Sci.*, 2016, **7**, 896–904; (b) S.-T. Pham, K. Ikemoto, K. Z. Suzuki, T. Izumi, H. Taka, H. Kita, S. Sato, H. Isobe and S. Mizukami, Magneto-electroluminescence Effects in The Single-layer Organic Light-emitting Devices with Macrocyclic Aromatic



Hydrocarbons, *APL Mater.*, 2018, **6**, 026103; (c) K. Ikemoto, M. Akiyoshi, A. Kobayashi, H. Kita, H. Taka and H. Isobe, Optimising Reaction Conditions in Flasks for Performances in Organic Light-emitting Devices, *Chem. Sci.*, 2025, **16**, 3045–3050.

19 In our previous study (ref. 13), enantiomers of phenine monopolluxene were designated as (*P*)- and (*M*)-isomers to describe the overall helical structure comprising triple helix of three arms. In this study, we found it better to designate the helicity of each arm to describe the molecular structure in a more precise manner. With the system adopted in the present study, the enantiomers of monopolluxenes are designated as (*P,P,P*)- and (*M,M,M*)-isomers.

20 H. A. Favre and W. H. Powell, *Nomenclature of Organic Chemistry: IUPAC Recommendations and Preferred Names 2013*, Royal Society of Chemistry, 2013.

21 (a) S. Sato, A. Unemoto, T. Ikeda, S. Orimo and H. Isobe, Carbon-rich Active Materials with Macroyclic Nanochannels for High-capacity Negative Electrodes in All-solid-state Lithium Rechargeable Battery, *Small*, 2016, **12**, 3381–3387; (b) T. Matsuno and H. Isobe, Trapped Yet Free Inside The Tube: Supramolecular Chemistry of Molecular Peapods, *Bull. Chem. Soc. Jpn.*, 2023, **96**, 406–419.

22 S. R. Batten and R. Robson, Interpenetrating Nets: Ordered, Periodic Entanglement, *Angew. Chem., Int. Ed.*, 1998, **37**, 1460–1494.

23 L. Carlucci, G. Ciani, D. M. Proserpio and A. Sironi, A Three-Dimensional ‘Racemate’. Interpenetration of Two Enantiomeric Networks of the SrSi₂ Topological Type in the Polymeric Complex [Ag₂(2,3-Me₂pyz)₃][SbF₆]₂ (2,3-Me₂pyz = 2,3-dimethylpyrazine), *Chem. Commun.*, 1996, 1393–1394.

24 V. Luzzati, A. Tardieu, T. Gulik-Krzywicki, E. Rivas and F. Reiss-Husson, Structure of the Cubic Phases of Lipid-Water Systems, *Nature*, 1968, **220**, 485–488.

25 C. J. Kepert, T. J. Prior and M. J. Rosseinsky, A Versatile Family of Interconvertible Microporous Chiral Molecular Frameworks: The First Example of Ligand Control of Network Chirality, *J. Am. Chem. Soc.*, 2000, **122**, 5158–5168.

26 We believe that the yield of **1** from arylboronic acid **5** was low because of low solubility of **5** and formation of interpenetrated boroxine.

27 (a) K. Takaba, S. Maki-Yonekura, S. Inoue, T. Hasegawa and K. Yonekura, Protein and Organic-Molecular Crystallography with 300kV Electrons on a Direct Electron Detector, *Front. Mol. Biosci.*, 2021, **7**, 612226; (b) H. Kurokawa, S. Maki-Yonekura, K. Takaba, T. Higashino, S. Inoue, T. Hasegawa and K. Yonekura, 3D Electron Diffraction Structure of an Organic Semiconductor Reveals Conformational Polymorphism, *J. Am. Chem. Soc.*, 2025, **147**, 5669–5678.

28 K. Yonekura, S. Maki-Yonekura, H. Naitow, T. Hamaguchi and K. Takaba, Machine Learning-Based Real-Time Object Locator/Evaluator for Cryo-EM Data Collection, *Commun. Biol.*, 2021, **4**, 1044.

29 A. L. Korich and P. M. Iovine, Boroxine Chemistry and Applications: A Perspective, *Dalton Trans.*, 2010, **39**, 1423–1431.

30 (a) S. Sato, A. Yoshii, S. Takahashi, S. Furumi, M. Takeuchi and H. Isobe, Chiral Intertwined Spirals and Magnetic Transition Dipole Moments Dictated by Cylinder Helicity, *Proc. Natl. Acad. Sci. U. S. A.*, 2017, **114**, 13097–13101; (b) Z. Sun, T. Matsuno and H. Isobe, Stereoisomerism and Structures of Rigid Cylindrical Cycloarylenes, *Bull. Chem. Soc. Jpn.*, 2018, **91**, 907–921.

31 B. Chen, R. Hoffmann, N. W. Ashcroft, H. Badding, E. Xu and V. Crespi, *J. Am. Chem. Soc.*, 2015, **137**, 14373–14386.

32 (a) CCDC 2486579: Experimental Crystal Structure Determination, 2025, DOI: [10.5517/ccdc.csd.cc2pgh7x](https://doi.org/10.5517/ccdc.csd.cc2pgh7x); (b) CCDC 2486580: Experimental Crystal Structure Determination, 2025, DOI: [10.5517/ccdc.csd.cc2pgh8y](https://doi.org/10.5517/ccdc.csd.cc2pgh8y).

